JOURNAL OF THEORETICAL
AND APPLIED MECHANICS
46, 2, pp. 443-455, Warsaw 2008

EXPERIMENTAL VERIFICATION OF A METHOD OF FINAL POSITIONING OF A LOAD FOR ROTARY CRANES

Andrzej Maczyński
Jerzy Płosa

Department of Mechanics and Computer Methods, University of Bielsko-Biała, Poland
e-mail: amaczynski@ath.bielsko.pl; jplosa@ath.bielsko.pl

In the paper, a method of final positioning of a load in slewing motion for jib cranes is proposed. The method is based on the so called "map of basic functions". The map stores drive functions of jib slewing motion for particular slew angles chosen so that they form a kind of base. The basic functions are determined for certain operational parameters (angle of jib slew, time of slewing, crane radius, mass of the load, length of the rope, etc.) using optimisation methods. Drive functions for different parameters, particularly for different slew angles, are calculated by a crane control system directly before slewing. Linear interpolation is used for this task. The method proposed has been experimentally verified using a physical model of a jib crane.

Key words: crane, positioning, experimental investigation

1. Introduction

Final positioning of a crane load in slewing motion means that at the end of jib motion the load should stay motionless at the desired point. In real conditions, this is difficult to achieve, but any significant limitation of final load oscillations is welcome. Immobility of the load after slewing motion enables next operations to be performed immediately by the operator. Effectiveness of reload and assembly works and the level of both active and passive safety also increases.

The problem of load positioning of jib cranes was considered by many authors (Hara *et al.*, 1989; Sakawa and Nakazumi, 1985; Sakawa *et al.*, 1981; Tanizumi *et al.*, 1994). Often, an application of hoisting drum motion or motion changing the crane radius simultaneously with slewing motion is proposed by Abdel-Rahman and Nayfeh (2002), Bednarski *et al.* (1997), Kłosiński (2000). Sometimes purposefulness of using additional mechatronical systems is discussed by Balachandran and Fang (1999), Maczyński (2005). A close-loop control system is assumed in the majority of proposed methods (Balachandran and Fang, 1999; Kłosiński, 2000) that are designed for cranes with high capacity. In this paper however, a simple method of final load positioning is presented. It has been developed for cheap, small cranes, e.g. pillar ones. In the method, an open-loop control system based on a so-called "map of basic slewing functions" is assumed. The slewing functions of the jib (called the drive functions from now on) for chosen slew angles and certain operation parameters are determined by means of optimisation. Those functions would be permanently stored in the crane control system (e.g. a PLC controller), forming the mentioned map. The optimisation is performed on a simplified crane model which ensures its significant numerical effectiveness. The drive functions for other, intermediate slew angles would be calculated by the control system directly before slewing by means of interpolation.

2. Dynamical model of a crane

The simplified crane model used for the optimisation task is presented in Fig. 1. It is assumed that the supporting structure, rope system and drives are non-deformable. The equations of motion of the load can be written as follows

$$
\begin{aligned}
m_L\ddot{x}_L &= S\frac{x_G - x_L}{L_L} \qquad\qquad m_L\ddot{y}_L = S\frac{y_G - y_L}{L_L} \\
m_L\ddot{z}_L &= S\frac{z_G - z_L}{L_L} - m_L g
\end{aligned}
\tag{2.1}
$$

where

m_L	–	mass of the load
$\boldsymbol{r}_L$	–	vector of coordinates of the load, $\boldsymbol{r}_L = [x_L, y_L, z_L]^\top$
$\boldsymbol{r}_G$	–	vector of coordinates of the point G (head of the jib), $\boldsymbol{r}_G = [x_G, y_G, z_G]^\top$
L_L	–	length of the rope within the segment GL
S	–	force in the rope
φ	–	slew angle of the jib
ψ	–	jib slope angle.

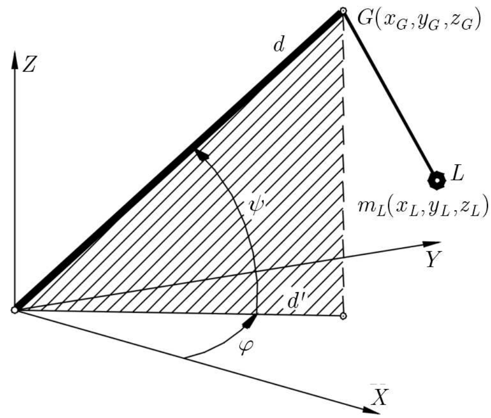

Fig. 1. Simplified model of a crane used for the optimisation task

There are four unknowns x_L, y_L, z_L, S in these equations, and thus an additional constraint equation is necessary

$$L_L^2 = |GL|^2 = (x_G - x_L)^2 + (y_G - y_L)^2 + (z_G - z_L)^2 = \text{const} \tag{2.2}$$

The force S can be calculated from the formula

$$\begin{aligned} S = \frac{m_L}{L_L}\Big[g(z_G - z_L) + (\dot{x}_G - \dot{x}_L)^2 + (\dot{y}_G - \dot{y}_L)^2 + (\dot{z}_G - \dot{z}_L)^2 + \\ + \ddot{x}_G(x_G - x_L) + \ddot{y}_G(y_G - y_L) + \ddot{z}_G(z_G - z_L)\Big] \end{aligned} \tag{2.3}$$

With reference to Fig. 1, the following relations occur

$$\begin{aligned} x_G &= d\cos\psi\cos\varphi = d'\cos\varphi \qquad y_G = d\cos\psi\sin\varphi = d'\sin\varphi \\ z_G &= d\sin\psi = \text{const} \end{aligned} \tag{2.4}$$

Including equations (2.3) and (2.4) in equations (2.2) and (2.1), differential equations of motion for the simplified model of a crane are obtained.

3. Optimisation of drive functions

Let $\varphi_w(t)$ denote the drive function of jib slewing. It is assumed that for $t \in \langle t_0, T\rangle$, the function $\varphi_w(t)$ can be approximated by means of third-order spline functions (Fig. 2) and it can be expressed as follows

$$\varphi_w(t)\Big|_{t\in\langle t_{i-1},t_i\rangle} = a_i(t-t_{i-1})^3 + b_i(t-t_{i-1})^2 + c_i(t-t_{i-1}) + d_i \tag{3.1}$$

where

$t_i = \dfrac{T}{n_d} i$ for $i = 0,1,\dots,n_d$

a_i, b_i, c_i, d_i – coefficients

n_d – number of sections into which the time interval $\langle t_0, T\rangle$ has been divided.

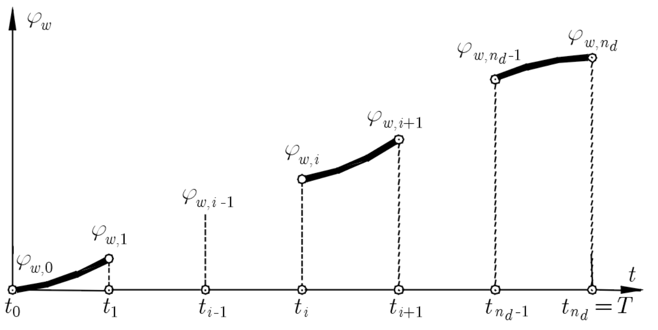

Fig. 2. Function $\varphi_w(t)$ approximated by spline functions

As the decisive variables in the optimisation task, components of the vector below have been assumed.

Components of the following vector

$$\boldsymbol{X} = [\varphi_{w,1}, \varphi_{w,2}, \dots, \varphi_{w,n_d-1}]^\top \tag{3.2}$$

where $\varphi_{w,i} = \varphi_w(t_i)$ for $i = 1,2,\dots,n_d-1$, are chosen as the decisive variables for the optimisation task considered.

An objective function is defined in the form

$$F = C_1 \frac{m_L}{2} \boldsymbol{v}_{LT}^2 + C_2 \|\boldsymbol{r}_{LT} - \boldsymbol{r}_{LF}\|^2 \tag{3.3}$$

where

$\boldsymbol{r}_{LT} = \boldsymbol{r}_L|_{t=T}, \boldsymbol{v}_{LT} = \boldsymbol{v}_L|_{t=T}$ – vector of coordinates and velocity of the load for $t = T$

$\boldsymbol{r}_{LF}$ – vector of desired coordinates of the load for $t = T$

C_1, C_2 – coefficients (weights).

The objective function defined above means that one can expect that at the end of slewing motion the load is at a particular point in space and furthermore its kinetic energy is minimal. Therefore, precise formulation of the optimisation task can be expressed in the following terms: *find the minimum of the functional F presented by equation (3.3) by selection of values $\varphi_{w,1},\dots,\varphi_{w,n_d-1}$ that are components of the vector $\boldsymbol{X}$ (in definition (3.2)).* The problem of optimisation considered here is a problem without constraints. The Nelder-Meads method (Wit, 1986) has been used for its solution. Like most optimisation methods, this one is also sensitive to a selection of the initial approximation. In the paper, it is assumed that the initial approximation of the vector $\boldsymbol{X}$

$$\boldsymbol{X}_0 = [\varphi_{w,1,0},\dots,\varphi_{w,n_d-1,0}]^\top \tag{3.4}$$

is obtained based upon the formulae

$$\varphi_{w,i,0} = \varphi_w(t_i) = \begin{cases} \dfrac{8\varphi_{w,max}}{T^4}t^3(-t+T) & \text{when} \quad t \leqslant \dfrac{T}{2} \\ \dfrac{8\varphi_{w,max}}{T^4}(t-T)^3t + \varphi_{w,max} & \text{when} \quad t > \dfrac{T}{2} \end{cases} \tag{3.5}$$

where $\varphi_{w,max}$ is the final angle of slewing motion.

This function fulfills the following conditions

$$\begin{aligned} &\varphi_w(0) = 0 && \dot{\varphi}_w(0) = 0 \\ &\varphi_w\Big(\frac{T}{2}\Big) = \frac{1}{2}\varphi_{w,max} \\ &\varphi_w(T) = \varphi_{w,max} && \dot{\varphi}_w(T) = 0 \end{aligned} \tag{3.6}$$

The thus chosen function makes it possible that courses of $\varphi_w = \varphi_w(t)$ and $\dot{\varphi}_w = \dot{\varphi}_w(t)$ curves are smooth.

Values of the coefficients C_1 and C_2 (Eq. (3.3)) are determined during numerical simulations. The main criterion of this determination is the best quality of the load positioning at the end of slewing motion.

4. Determination of the drive functions for intermediate angles of slewing

In this part of the paper, intermediate angles of slewing mean angles belonging to an interval determined by base angles. Determination of drive functions for an intermediate angle will be presented in an example. Let us assume that drive functions for two basic slew angles are known, e.g. for $60°$ and $90°$.

These functions are shown in Fig. 3 respectively as the black and the grey line. They have been calculated according to the method discussed in Section 3. For these functions, the forms of vectors of decisive variables (3.2) obtained as a result of the optimisation task are known. In Fig. 3, the marks (squares) placed on suitable curves correspond with elements of these vectors. In the first step linear interpolation is used to determine the time of motion T_k for a required (intermediate) slew angle (in our example for $75°$).

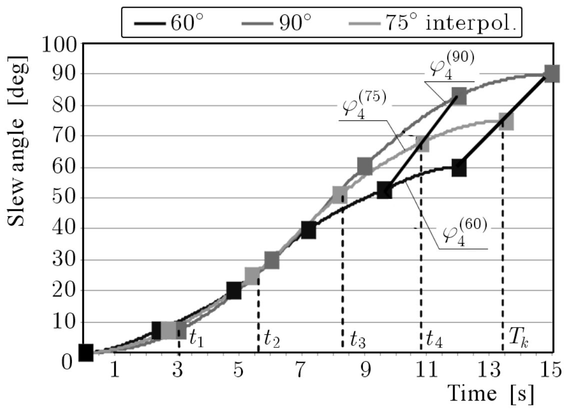

Fig. 3. Example of definition of the drive function for an intermediate slew angle

Next, the time interval $\langle 0, T_k \rangle$ is divided into n_d sections (in the example: $n_d = 5$) and values of the time t_i are determined according to

$$t_i = \frac{T_k}{n_d} i \qquad\qquad i = 0, 1, \ldots, n_d$$

Using once more the interpolation and knowledge of decisive variables for basic angles $60°$ and $90°$, values of the "partial" angles for $t_1, \ldots, t_{n_\varphi - 1}$ and the slew angle of $75°$ can be calculated. Figure 3 presents geometrical interpretation of determination of the "partial" angle for $t_i = t_4$. The set of partial angles obtained in this way is an equivalent of the vector of decisive variables in the optimisation task. Similarly as for the basic angles, the continuous form of the drive function, thus the relationship $\phi_w = \phi_w(t)$, can be expressed using spline functions.

5. Experimental stand

The proposed method of final load positioning in slewing motion has been experimentally verified on a physical model. A schematic diagram of the test stand is presented in Fig. 4. A photograph of the stand is shown in Fig. 5. The model of a jib crane is the main part of the stand. Elements of the Sandia manipulator owned by the Department of Mechanics and Computer Engineering Methods, University of Bielsko-Biała, have been used to build the stand. The jib (element 4 in Figs. 4 and 5), made of aluminium, close profile is fixed to the manipulator pedestal (element 3 in Figs. 4 and 5). The jib can be fixed at three different angles. The rope (element 6 in Figs. 4 and 5) with a steel ball (element 5 in Figs. 4 and 5) modelling the load is suspended at the end of the jib. The point of suspension can be freely moved along the jib.

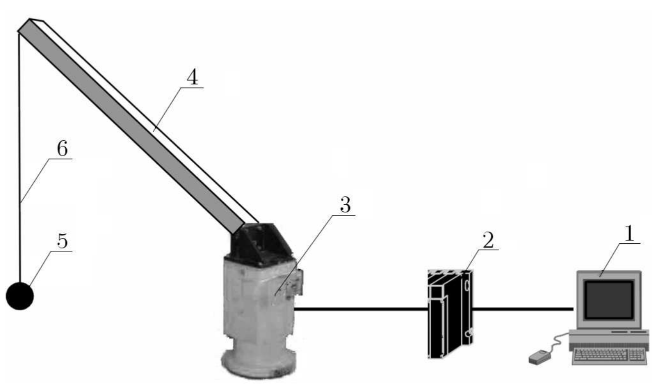

Fig. 4. Schematic diagram of the test stand; 1 – PC with "Test Point" software and DA card, 2 – controller, 3 – manipulator pedestal with servo-motor, gear and rate generator, 4 – jib, 5 – load, 6 – rope

The slew of the manipulator pedestal and, simultaneously, the slew of the jib are realized by means of a brushless, direct-current RTM ct type servo-motor with three-phase winding and six poles. This motor is provided with a brushless, direct-current rate generator with the Hall rotor position sensors. This generator is used in the control system of electronic commutation. Speed of the motor (max 4000 r.p.m.) is reduced by harmonic gear type HDUC with the transmission ratio 1:158. Control of speed of the brushless motors relies on changing the time duration (length) of a current impulse (Tunia, 1983). Such motors are commonly used in CNC machines and manipulators.

Figure 6 shows a diagram of the control system of motor speed. The main elements of the control system are: "Test Point" software, digital-analogue

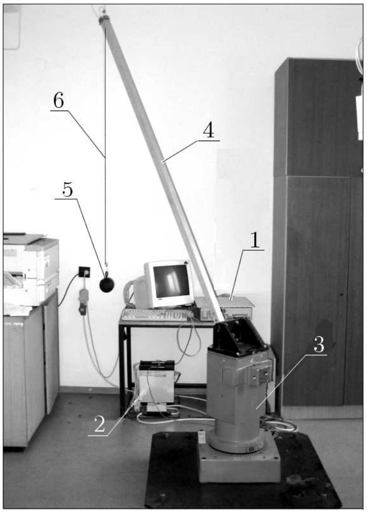

Fig. 5. Photograph of the test stand

card DA, controller, motor and direct-current rate generator. The software "Test Point" ver. 3.1 and the digital-analogue Keithley DAS 1802 HR-DA card have been installed on a PC (element 1 in Figs. 4 and 5). As a controller, the transistor controller SYD 106 TH (element 2 in Figs. 4 and 5) has been applied. This control system of motor speed enables realization of different forms of kinematic inputs.

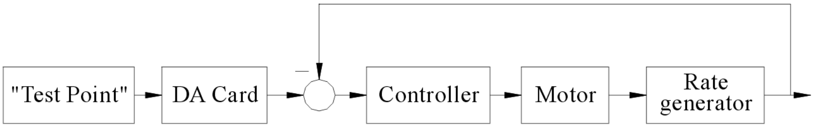

Fig. 6. Diagram of the control system of motor speed

The "Test Point" software is a professional object-oriented system which leverages multi-threading capabilities of operating systems. It enables:

- I/O services for analogue and digital cards,
- data analysis, filtration and conversion,
- graphical presentation of data.

It can be useful for control or diagnostics (monitoring) of various processess in industry and research laboratories. In the present investigation, special application has been compiled in the "Test Point" software. The application enables a file to be read with a desired time course of rotational speed of the motor and a suitable digital signal to be generated. Because drive functions determined according to Sections 3 and 4 prescribe the time courses of slew angles of the jib, they have to be first recalculated onto corresponding rotational speeds of the motor.

The signal generated by the "Test Point" application is converted by the digital-analogue card DAS 1802 HR-DA to an analogue signal (voltage). The voltage from the DA card is used by the transistor controller SYD 106 TH. It is a special PID controller designed for speed control of brushless motors. The signal from the rate generator is also the input to the controller. Replaceable resistors and capacitors (installed on the controller) have been matched to the motor at the Electrotechnical Institute in Warsaw.

6. Experimental investigations

The experimental investigations presented in the paper were carried out for the following parameters: length of the jib (dimension d in Fig. 1) 2.243 m, mass of the load 3.25 kg, length of the rope 1.61 m, angle of jib slope 57.5°. The experiments were performed for inputs listed in Table 1.

Table 1

	Slew angle	Duration of motion [s]	Drive functions
1	70°	4.1	a) function according to formula (3.5) b) optimised function
2	90°	4.4	a) function according to formula (3.5) b) optimised function
3	80°	4.3	a) function according to formula (3.5) b) optimised function c) interpolated function

Graphs in Figs. 7a,b present time courses of the optimised drive functions of jib slewing and the functions determined according to initial approximation formula (3.5), respectively for 70° and 90°. Figure 7c shows the drive functions for the slew angle of 80° and, additionally, the function determined according to Section 4.

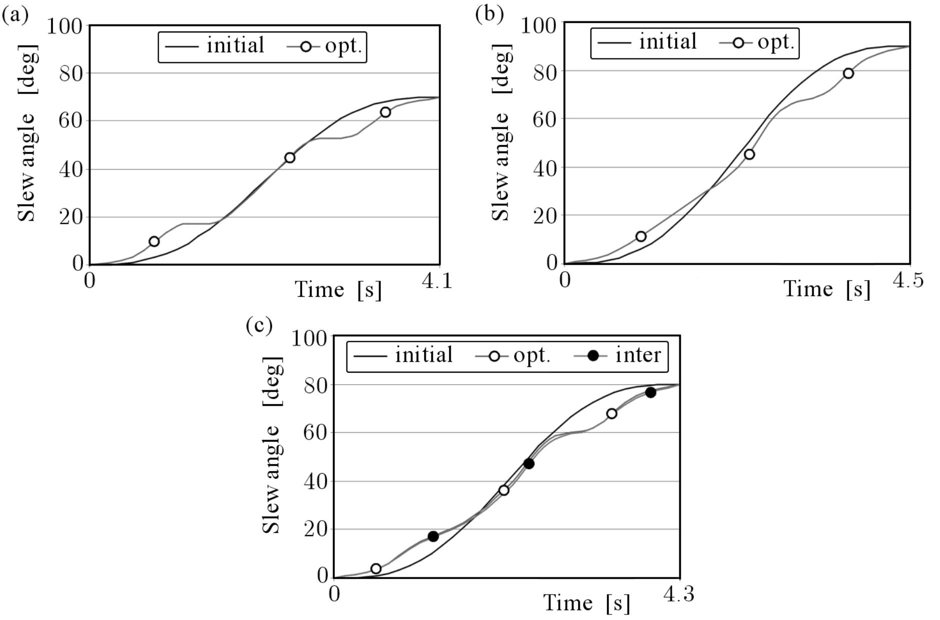

Fig. 7. Drive function for angle: (a) – 70°, (b) – 90°, (c) – 80°

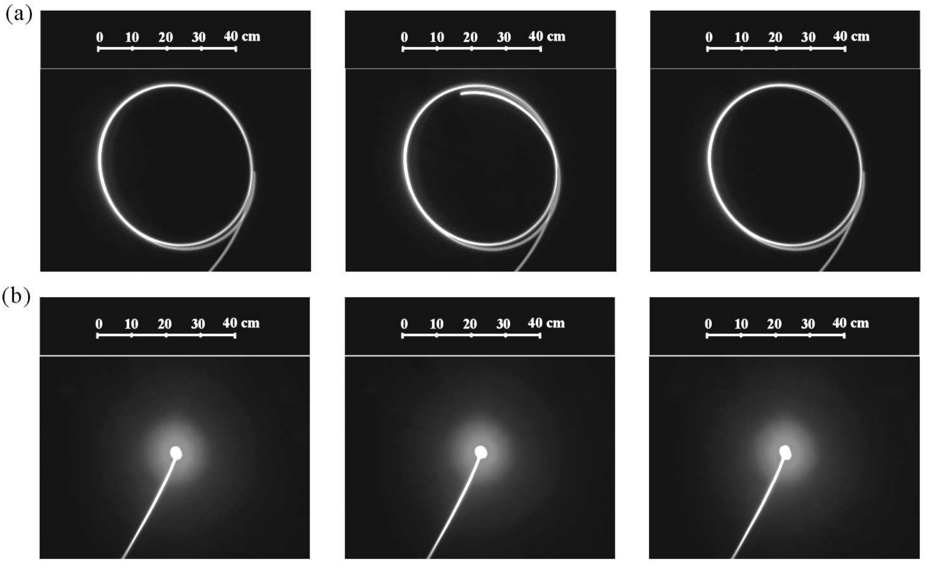

Fig. 8. Experimentally recorded final part of load trajectory for slew of 70° and drive function calculated according to (3.5): (a) – case 1a, (b) – case 1b

(a)
(b)
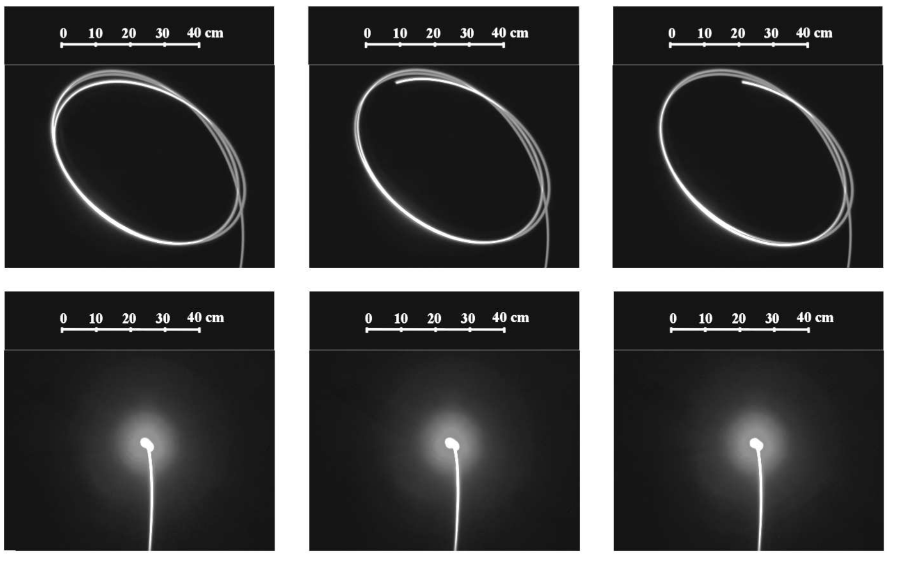

Fig. 9. Experimentally recorded final part of load trajectory for slew of $90°$ and drive function calculated according to (3.5): (a) – case 2a, (b) – case 2b

Figures 8-10 present courses of load trajectories (final parts) for the analysed cases of the jib slewing registered by means of a digital camera. The time of exposure was 8 s. The position of a red LED mounted in the centre of the load was traced in these photographs. Three frames were executed for each case in order to confirm reproducibility of the obtained results.

7. Summary

The obtained experimental results prove significant effectiveness of the proposed method of the final load positioning in slewing motion of a jib crane. This statement involves both basic and intermediate angles. It is important to note that in the presented experiment, the basic functions have been calculated fairly infrequently – the step between them is $20°$. The courses from photographs show that final load oscillations have been reduced from nearly 50 cm down to about 4 cm in each analysed case.

Because the method requires only an open-loop control system, it can be recommended for final load positioning in simple rotary cranes, e.g. pillar or wall cranes. It can be also used in the case of small mobile cranes.

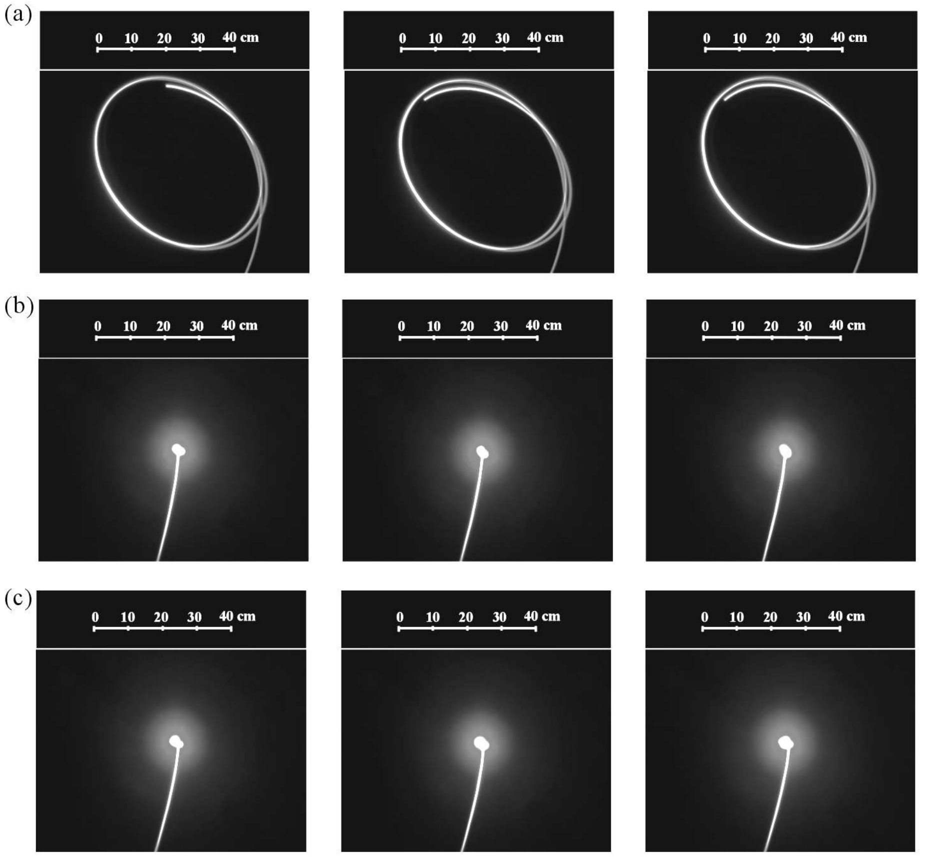

Fig. 10. Experimentally recorded final part of load trajectory for slew of $80°$ and drive function calculated according to (3.5): (a) – case 3a, (b) – case 3b, (c) – case 3c

References

1. Abdel-Rahman E.M., Nayfeh A.H., 2002, Pendulation reduction in boom cranes using cable length manipulation, *Nonlinear Dynamics*, **27**, 3, 255-269

2. Balachandran B., Li Y.-Y., Fang C.-C., 1999, A mechanical filter concept for control of non-linear crane-load oscillations, *Journal of Sound and Vibration*, **228**, 3, 651-682

3. Bednarski S., Cink J., Tomczyk J., 1997, Pozycjonowanie ładunku w ruchu roboczym żurawia portowego, *Proc. X Konferencji Problemy Rozwoju Maszyn Roboczych*, part I, 25-31

4. Hara K., Yamamoto T., Kobayashi A., Okamoto M., 1989, Jib crane control to suppress load swing, *International Journal of Systems and Science*, **20**, 5, 715-731

5. Kłosiński J., 2000, Sterowanie ruchami roboczymi żurawi samojezdnych zapewniające pozycjonowanie przenoszonego ładunku, *Zeszyty Naukowe Politechniki Łódzkiej Filii w Bielsku-Białej, Rozprawy naukowe*, **35**, 55, Rozprawa habilitacyjna, Bielsko-Biała

6. Maczyński A., 2005, *Pozycjonowanie i stabilizacja położenia ładunku żurawi wysięgnikowych*, Wydawnictwo ATH, Seria Rozprawy Naukowe, Nr 14, Bielsko-Biała

7. Sakawa Y., Nakazumi A., 1985, Modeling and control of a rotary crane, *Journal of Dynamic Systems, Measurement and Control*, **107**, 200-206

8. Sakawa Y., Shindo Y., Hashimoto Y., 1981, Optimal control of a rotary crane, *Journal of Optimization Theory and Applications*, **35**, 4, 535-557

9. Tanizumi K., Hino J., Yoshimura T., Sakai T., 1994, Modelling of dynamic behaviour and control of truck cranes with hydraulic system in swing operation, *Transactions of the Japan Society of Mechanical Engineering*, Part 6, **20**, 1262-1277

10. Tunia H., 1983, *Podstawy automatyki napędu elektrycznego*, PWN Warszawa

11. Wit R., 1986, *Metody programowania nieliniowego. Minimalizacja funkcji gładkich*, WNT Warszawa

Eksperymentalna weryfikacja metody końcowego pozycjonowania ładunku żurawi obrotowych

Streszczenie

W pracy przedstawiono metodę końcowego pozycjonowania ładunku żurawi wysięgnikowych w ruchu obrotowym. Bazuje ona na tzw. mapie funkcji bazowych, w której zapamiętywane są funkcje napędowe obrotu nadwozia dla wybranych "bazowych" kątów obrotu. Funkcje te wyznaczane są na drodze optymalizacji dla określonych parametrów eksploatacyjnych (kąt obrotu nadwozia, czas obrotu, wysięg, masa ładunku, długość liny). Funkcje napędowe dla innych parametrów, w szczególności dla inny kątów obrotu, obliczane są przez układ sterujący bezpośrednio przed rozpoczęciem ruchu. W tym celu stosowana jest interpolacja liniowa. Proponowana metoda została zweryfikowana eksperymentalnie na stanowisku badawczym.

Manuscript received May 7, 2007; accepted for print January 18, 2008